Pergamon

Tetrahedron 58 (2002) 8811–8823

TETRAHEDRON

α-Amino acids and dioxopiperazines crowned at the α-carbons with polyether macrorings. Synthesis, complexation and self-assembling properties

Martin Bělohradský,[a] Ivana Císařová,[b] Petr Holý,[a] Jan Pastor[a] and Jiří Závada[a,*]

[a]*Institute of Organic Chemistry and Biochemistry, Academy of Sciences of the Czech Republic, 166 10 Prague, Czech Republic*
[b]*Department of Inorganic Chemistry, Charles University, 128 40 Prague, Czech Republic*

Received 7 May 2002; revised 1 August 2002; accepted 22 August 2002

Abstract—Crowned α-amino acids **7a–c** and their dioxopiperazine derivatives **12a–c** were prepared from the easily accessible masked tris(hydroxymethyl)aminomethane **1**. X-Ray crystal structures of the free as well as alkali metal ion coordinated compounds were investigated.

1. Introduction

Amino acids, being one of the fundamental constituents of the living matter, serve a central role in biology and chemistry. In addition to a limited number of proteinogenic amino acids, a much greater number of naturally occurring non-proteinogenic amino acids has been isolated. In spite of this abundant natural pool, the design of synthetic amino acids has emerged as a highly significant endeavor.

Many of the important properties and functions of amino acids and their derivatives depend on their hydrogen bonding capability. Now we have designed new amino acids and their dioxopiperazine derivatives that combine the potential for hydrogen bonding with the well-known metal ion coordinating capacity of macrocyclic polyethers (crowns).[1] Earlier, several such hybrid compounds have been already prepared[2a,c] and a remarkable propensity to self-assembly leading to a microporous architecture has been in one instance reported.[2c] Interest in this challenging topic[3] also underlies the novel design which rests on the 'crowning' of the α-carbon of glycine with a methylene–oligo(oxyethylene)–oxymethylene chain. A simultaneous anchoring of the crown, amino and carboxyl groupings at a single carbon atom has not been previously explored; its consequences upon the self-assembling properties of the resulting amino acids, their derivatives and alkali metal ion complexes are the subject of the present study.

Keywords: crown ethers; amino acids and derivatives; X-ray crystal structures.

* Corresponding author. Fax: +4202-3333-1733; e-mail: zavada@uochb.cas.cz

2. Results and discussion

2.1. Synthesis

The easily accessible[4] masked tris(hydroxymethyl)aminomethane **1** has been employed as the key building unit in the modular synthesis of the crowned amino acids **7a–c** (Scheme 1). Treatment of **1** with an appropriate oligo(oxyethylene)glycol ditosylate **2a–c** afforded the macrocyclic oxazolidines **3a–c** employing either NaH/THF (**3a**) or KOH/dioxane (**3b** and **3c**) in the Williamson synthesis. Acidic hydrolysis of the oxazolidines **3a–c**, followed by an in situ selective carbonylbenzyloxy (Cbz) reprotection of the resulting amino alcohols **4a–c** gave the carbamates **5a–c**. Their oxidation with the catalytic TEMPO–NaClO tandem[5] led to Cbz-protected amino acids **6a–c** which on reaction with diazomethane afforded methyl esters **8a–c**. The subsequent hydrogenolysis of **6a–c** and **8a–c** on Pd/C yielded smoothly the free amino acids **7a–c** and the deprotected esters **9a–c**, respectively.

The corresponding dioxopiperazines **12a–c** were prepared (Scheme 2) from the Cbz-protected amino acids **6a–c** and the deprotected methyl esters **9a–c** using benzotriazol-1-yl-oxy-tripyrrolidinophosphonium hexafluorophosphate (PyBOP). The intermediary Cbz-dipeptides **10a–c** were hydrogenolytically deprotected and the resulting dipeptide esters **11a–c** were converted into the target compounds **12a–c** on treatment with a methanolic solution of ammonia.

2.2. FAB MS screening of alkali metal ion complexation

The formation of alkali metal ion complexes from the crowned amino acids **7a–c** was monitored by FAB

0040–4020/02/$ - see front matter
PII: S0040-4020(02)01065-7

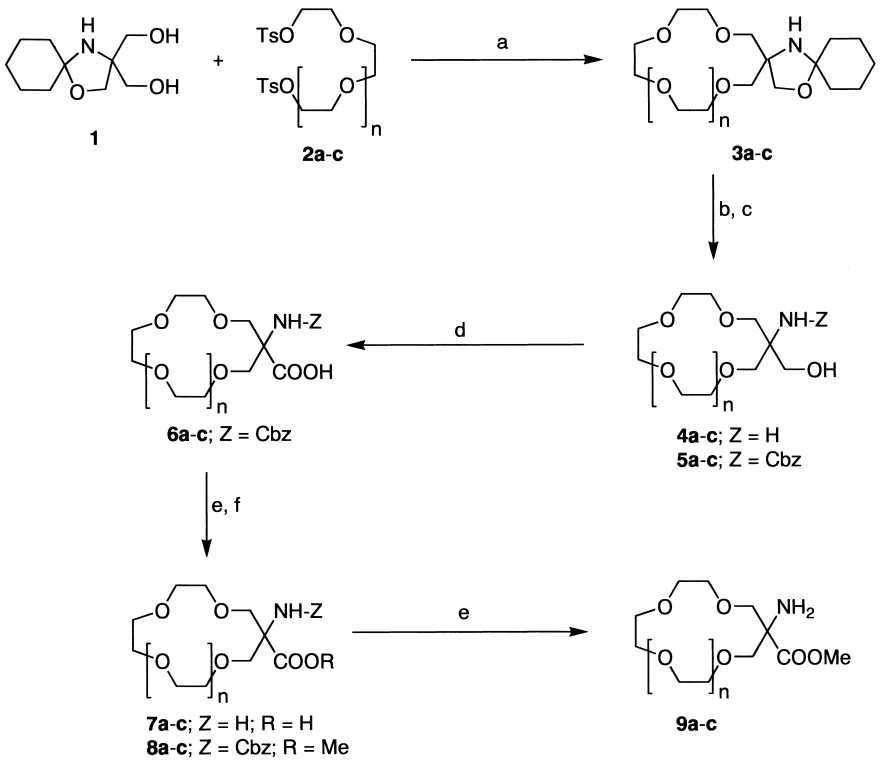

Scheme 1. (a) KOH, dioxane, 80°C, 20 h; yields 29–49%; (b) 3M HCl, 55°C, 5 h; not isolated; (c) CbzCl, $NaHCO_3$, H_2O/dioxane 1:1, 0°C, 4 h; yields 61–79%; (d) TEMPO, NaClO, $NaHCO_3$, CH_3CN/H_2O 1:1, 5 h; yields 70–80%; (e) 10% Pd/C, H_2, CH_3OH; yields 88–99%; (f) CH_2N_2, CH_2Cl_2, 15 min; yields 98–99%.

MS in a glycerol–thioglycerol matrix containing the appropriate ligand (1×10^{-2} M) and an equimolar mixture of alkali metal ions Li^+, Na^+, K^+, Rb^+, and Cs^+. The complexation was followed under acidic, neutral as well as basic conditions and the results are summarized in Table 1.

A cursory examination of the results immediately shows a qualitative accord with the known[1] crown cavity–alkali ion diameter relationship established for the parent (non-functionalized) series of crown compounds, with the sodium ion being preferentially complexed by the two smaller (**7a** and **7b**), whereas the potassium ion by the larger (**7c**) homologue. Noteworthy, the pH variation does not affect significantly the selectivity order, suggesting that the neighboring amino and carboxyl groupings do not participate in the intra-annular complex formation.

Irrespective of the pH variation, formation of 1:1 metal ion–crown complexes generally prevails under the standard (1:1) stoichiometric conditions. Upon a tenfold increase of the alkali metal ion concentration in the solution, however,

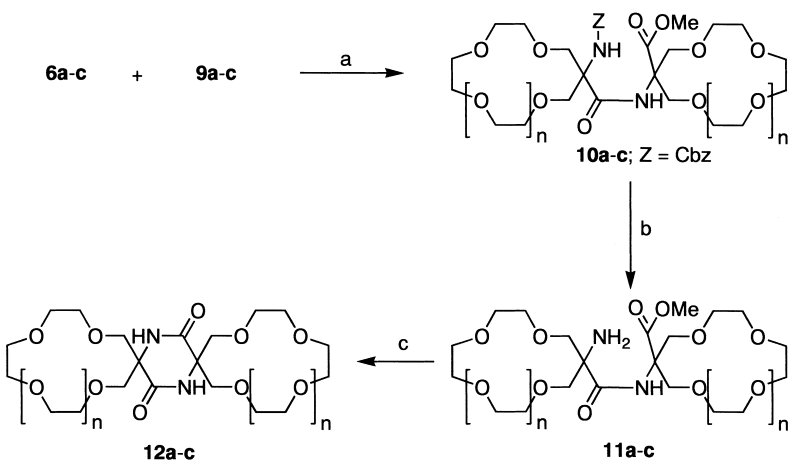

Scheme 2. (a) PyBOP, diisopropylethyl amine, CH_2Cl_2, 5 d; yields 61–73%; (b) 10% Pd/C, H_2, CH_3OH, 3 h; yields 92–97%; (c) NH_3, CH_3OH, 24 h; yields 40–64%.

Table 1. Relative abundance of alkali metal complexes from amino acids **7a**–**c** in FAB MS thioglycrol–glycerol matrix under acidic (A), neutral (N) and basic (B) conditions

	A			N			B		
	7a	**7b**	**7c**	**7a**	**7b**	**7c**	**7a**	**7b**	**7c**
Li^+	83	49	55	98	48	43	90	55	35
Na^+	100	100	76	100	100	63	100	100	30
K^+	92	62	100	92	52	100	89	52	100
Rb^+	58	42	57	57	30	43	50	30	35
Cs^+	63	52	55	61	30	40	50	30	25

For details see Section 4.3.

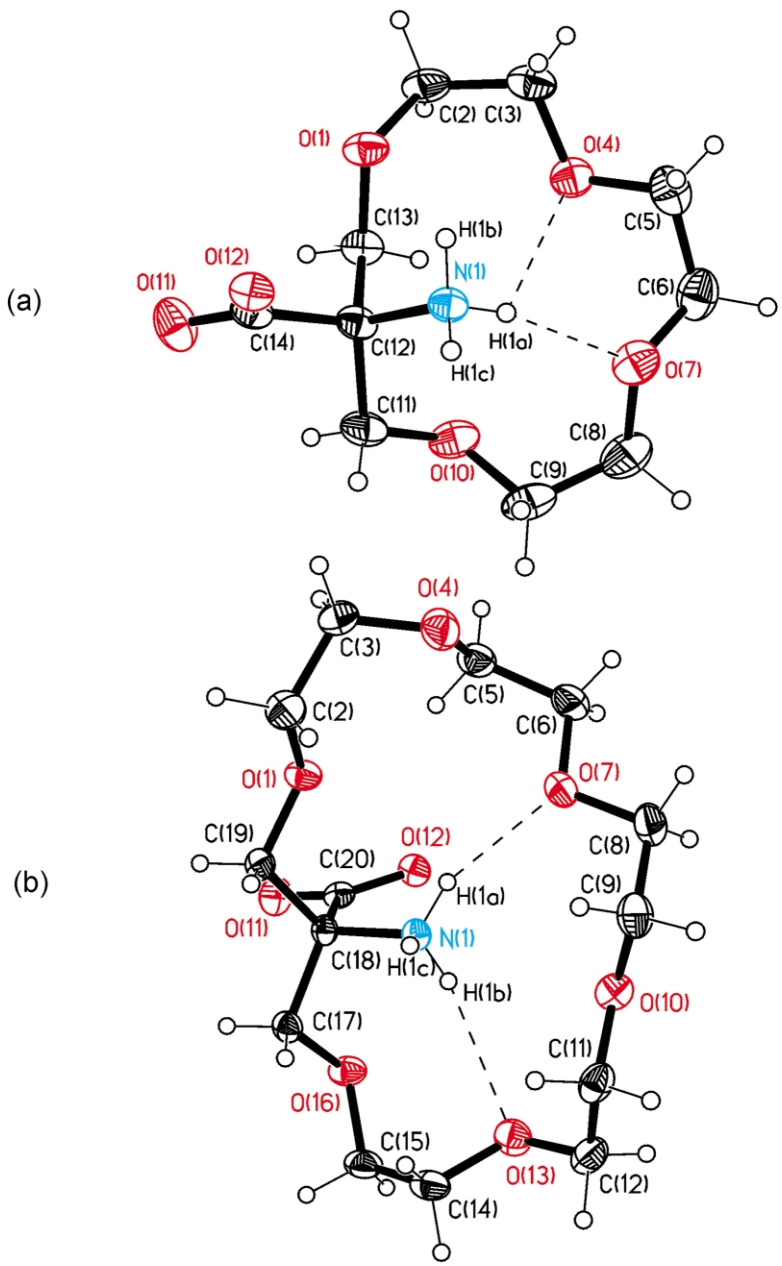

Figure 1. ORTEP drawings of the molecules of amino acid **7a** (a) and **7c** (b) with atom numbering (ellipsoids: 50% probability) and intramolecular hydrogen bonds (dashed lines).

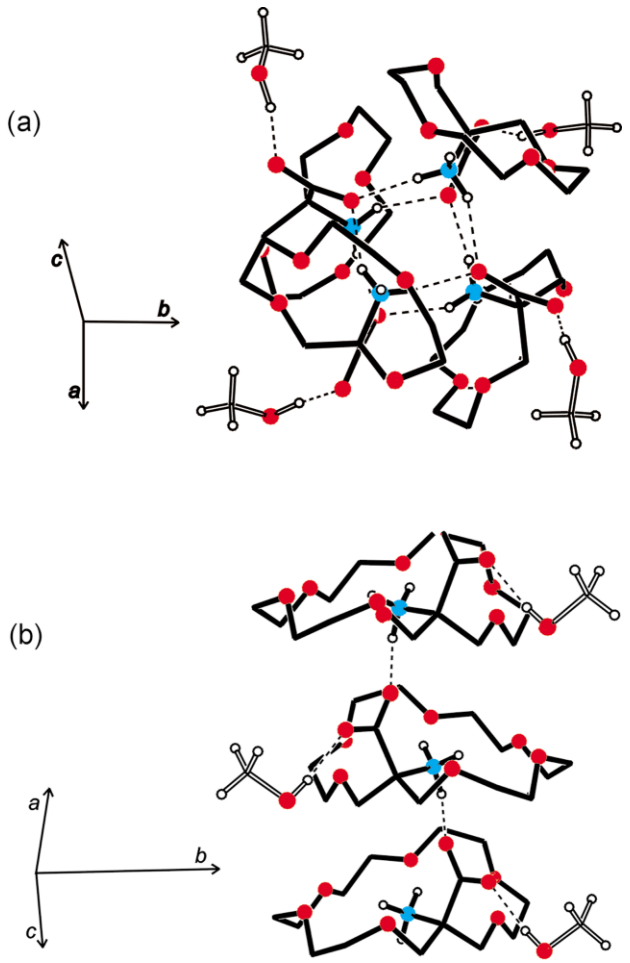

Figure 2. The cyclotetrameric vs. linear chain arrangement of molecules of amino acid **7a** (a) and **7c** (b) organized in the crystals by intermolecular hydrogen bonding. Carbon atoms are omitted and only intermolecular hydrogen bonds (dashed lines) are indicated. Atoms of oxygen and nitrogen are represented with red and blue circles, respectively.

2:1 metal ion–crown complexes become prominent in the FAB MS spectra, in particular under basic conditions. A simple rationale can be given in terms of an extra-annular salt formation.

2.3. X-Ray crystal structures

2.3.1. Crystal structure of the free amino acids 7a–c. Two of the three investigated free amino acids, **7a** and **7c**, afforded crystals suitable for X-ray diffraction analysis. Their molecular structure is largely unexceptional (Fig. 1(a) and (b), respectively); noteworthy is however the pattern of intramolecular and intermolecular hydrogen bonding.

In the amino acid **7a**, one of the three hydrogen atoms in the $-NH_3^+$ group participates in a bifurcated intramolecular hydrogen bond to the macrocyclic O(7) and O(4) oxygens (a shorter contact with O(7) and a longer one with O(4)). In the larger homologue **7c**, there is a pair of intramolecular hydrogen bonds connecting two hydrogens of the $-NH_3^+$ group with the macrocyclic O(7) and O(13) oxygen atoms.

The remaining hydrogen atoms at the $-NH_3^+$ group are available for participation in intermolecular hydrogen bonds. In each molecule of **7a**, two ammonium hydrogens are bonded with the carboxylate groups at the neighboring molecules. A single oxygen atom at each carboxylate group serves as an acceptor of two intermolecular hydrogen bonds donated from two distinct amino acid molecules giving rise to a cyclotetrameric arrangement of the amino acid **7a**. This is decorated at the corners of the supramolecular square by hydrogen bonding of the coordinatively unsaturated carboxy oxygens with four molecules of methanol (Fig. 2(a)).

In the crystal of **7c**, only one hydrogen at the $-NH_3^+$ pole is available for the intermolecular bonding with the carboxylate group, the result being an infinite linear chain (Fig. 2(b)).

2.3.2. Crystal structure of the metal ion coordinated amino acid 7b. Participation of the macrocyclic oxygens with the $-NH_3^+$ group in the intramolecular hydrogen bonds ceased upon intraannular co-ordination of the crowned amino acids **7a–c** with alkali metal ions, as evidenced by the crystal structure of the complex **7b**·NaCl (Fig. 3(a)). The sodium ion is coordinated by five oxygens which are placed in the central plane of the macroring. The equatorial pentaco-ordination of the sodium ion is complemented by the axial co-ordination with the chloride counterion and water molecule, residing, respectively, at the opposite apices of the pentagonal bipyramid. The sole direct contacts between the individual molecules **7b** are due to the intermolecular hydrogen bonds between the $-NH_3^+$ group and the macrocyclic oxygen (one bond per molecule). The weak direct contacts are supported by indirect contacts underlying the polymeric chains of the solvent-separated ion-pairs $\cdots H_2O\cdots Na^+\cdots X^-\cdots H_2O\cdots Na^+\cdots X^-\cdots$, in which chloride and carboxylate anions ($X{=}Cl^-$ and CO_2^-, respectively) alternate in the supramolecular network (Fig. 3(b)).

2.3.3. Crystal structure of the free dioxopiperazines 12a–c. Dioxopiperazines (DOP) represent robust building blocks (tectons) for self-assembly[6] into one-dimensional tapes organized by amidic double hydrogen bonds (Scheme 3, A). Recent studies by Whitesides and his co-workers[6b] indicated that this self-assembling pattern holds over a surprisingly wide range of DOP structure variation, including also alicyclic derivatives with small or common rings spiro-annelated in the α, α, α′, α′-positions. Significantly, the presence of other hydrogen bond donors and/or acceptors has been tolerated in some instances.[7] Extension of the tape pattern to the crowned DOP derivatives **12a–c** thus cannot be a priori ruled out. Model examination suggests that the self-assembled tapes **12a–c** could serve as a scaffold for an ordered stacking of the adjoined crown units (Scheme 3, B).

All three crowned DOP derivatives **12a–c** afforded suitable single crystals for X-ray diffraction analysis. Their molecular structure is depicted in Fig. 4(a)–(c). It may be seen that the central DOP ring in **12a–c** is invariably planar, whereas the appendant spiro-macrorings are non-planar, but approximately orthogonal with respect to the central ring, which is a prerequisite for the organized stacking. However, the

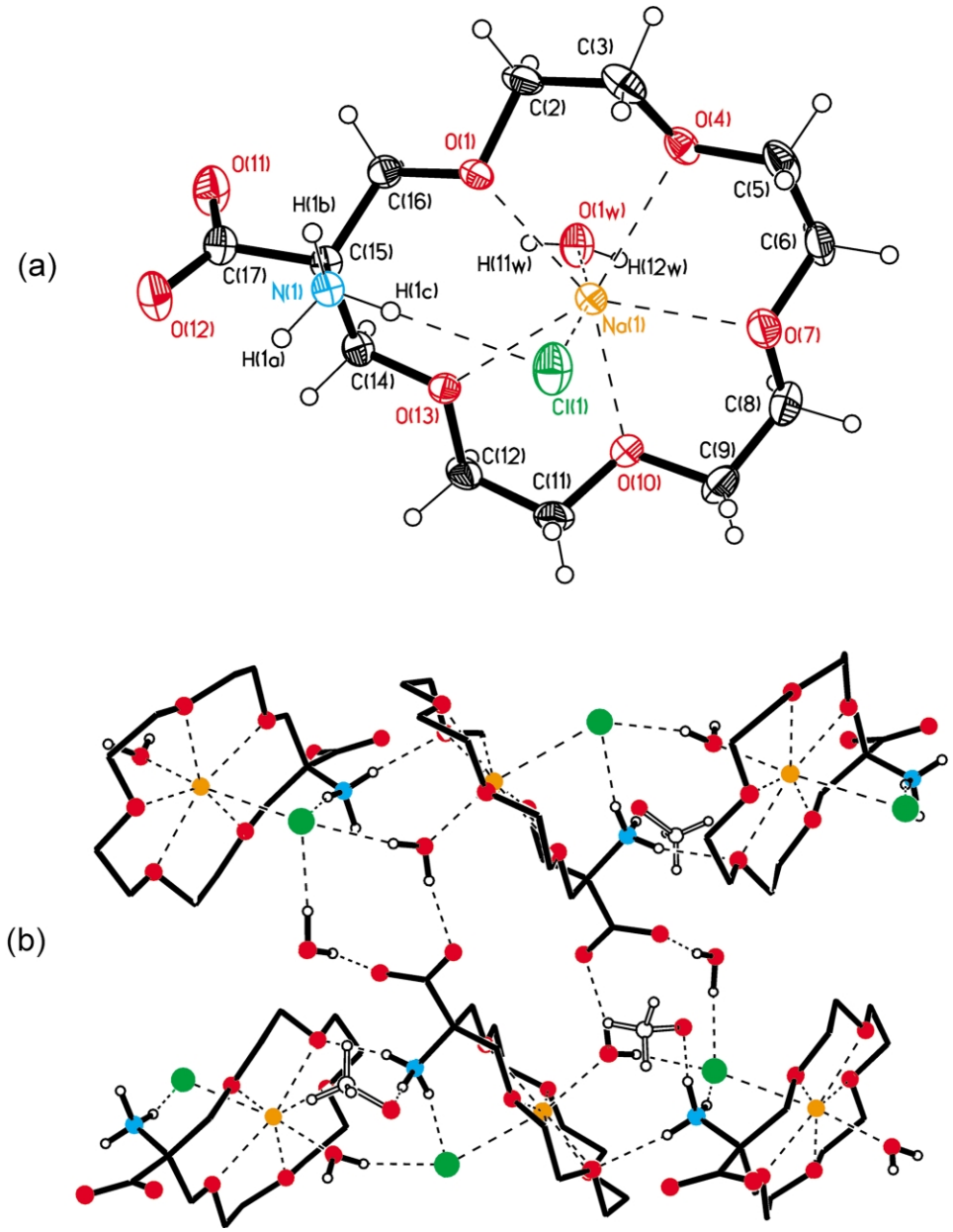

Figure 3. ORTEP drawing of the molecular structure (a) of the complex **7b**·NaCl with atom numbering (ellipsoids: 50% probability) and the crystal packing (b). Chloride anions and sodium cations are represented with green and orange circles, respectively. Red and blue circles represent oxygen and nitrogen atoms, respectively.

hydrogen-bonded tapes are absent in the crystals of all the three crowned homologues **12a**–**c**. Instead, a pair of intramolecular hydrogen bonds between the two amidic nitrogens at the central ring and the proximate (trans-annular) macrocyclic oxygens (Fig. 4(a) and (b), respectively) operates in the two smaller homologues **12a**, **b**. In the larger homologue **12c**, a molecule of water is moreover inserted into the intramolecular hydrogen bonds, allowing bifurcation towards two proximate oxygen atoms (Fig. 4(c)).

Interestingly, in spite of the missing hydrogen-bonded scaffold, eclipsed stacking of the individual tectons occurs in the crystals of **12a**–**c** giving rise to micropores (Fig. 5(a)–(c)). The filling of space appears to be the sole driving force behind this organization.

2.3.4. Crystal structure of the metal ion coordinated dioxopiperazine 12c. In order to probe the effect of metal ions on self-assembly of the crowned dioxopiperazines, crystal structure of the 1:1 complex **12c**·KSCN was examined.

In accord with expectations (cf. Section 2.3.2), the X-ray diffraction analysis shows that intramolecular hydrogen bonds have been suppressed upon the complexation; however, instead of the hydrogen-bonded tapes, a preferential co-ordination of the metal ion with the amidic carbonyl prevailed. As Fig. 6(a) shows, the potassium ion is coordinated with six macrocyclic oxygens lying in the central plane, but these equatorial contacts are accompanied by comparably close contacts with one amidic carbonyl and a solvent cluster, occupying the apices of a hexagonal

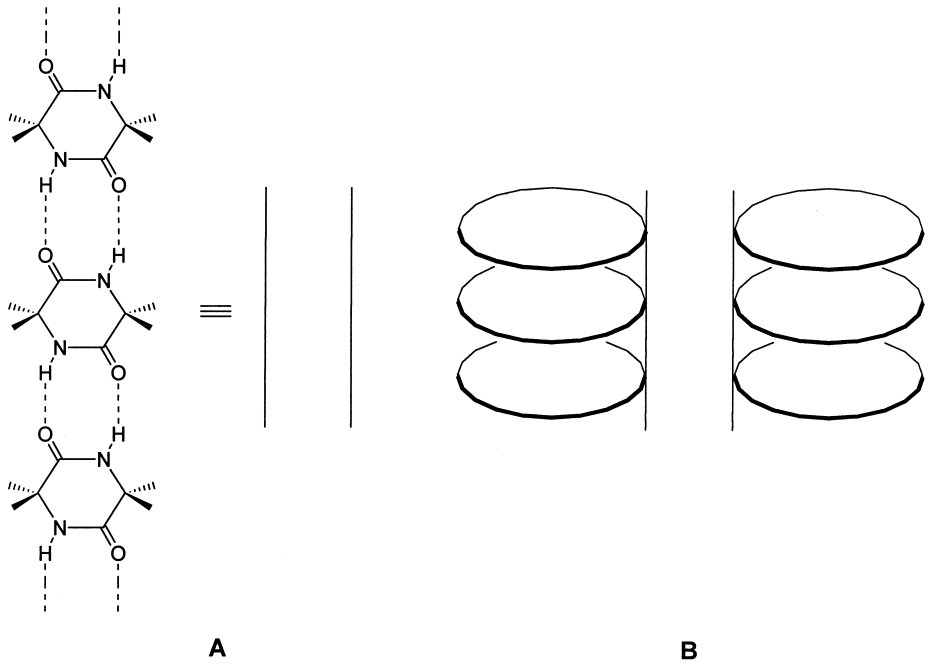

Scheme 3.

bipyramid; in this way the thiocyanide counterion is ousted from a direct coulombic interaction with the potassium cation.

Although intermolecular hydrogen bonding is thus relegated to a minor participation in the second co-ordination sphere, the eclipsed stacking of the individual tectons prevails again in the crystal giving rise to micropores (Fig. 6(b)).

3. Conclusions

To summarize, we have designed α-amino acids and dioxopiperazines 'crowned' at the α-carbons with a methylene–oligo(oxyethylene)–oxymethylene chain and proposed their modular synthesis. A remarkable propensity of the crown units to stacking under formation of micropores has been found in the crystals of the dioxopiperazine derivatives in the presence as well as in the absence of alkali metal ions.

4. Experimental

4.1. General remarks

^{1}H and ^{13}C NMR spectra were measured on FT NMR spectrometer Varian UNITY 500 (^{1}H at 500 MHz, 20°C, ^{13}C at 125.7 MHz, 40°C) in $CDCl_3$ and/or DMSO-d_6. Chemical shifts are referenced to the signal of solvent [δ (^{1}H) 2.50 and δ (^{13}C) 39.7]. FAB MS spectra were recorded with ZAB-EQ VG analytical instrument using a mixture of glycerol–thioglycerol matrix. Analytical samples were dried at 60°C/5 kPa for 24 h. TLC chromatography was performed on Kieselgel GF_{254} using Dragendorff spraying reagent. 2,2-Bis(hydroxymethyl)-1-aza-4-oxaspirodecane (**1**) and oligo(ethylene glycol) ditosylates (**2a**–**c**) were prepared according to known procedures.[4,8]

4.2. Synthetic procedures

4.2.1. Spiro-13-crown-4 (3a). A solution of **1** (18.6 g, 92 mmol) in dry THF (600 mL) and solution of tri(ethylene glycol)ditosylate (**2a**) (42.4 g, 92 mmol) in dry THF (600 mL) were added slowly (30 mL h^{-1}) to an intensively stirred suspension of NaH (9 g, 375 mmol) in dry THF (600 mL) under argon at reflux by dual syringe pump. Following 20 h reflux, about 2/3 of the solvent was distilled off, the reaction mixture was cooled and decomposed by dropwise addition of methanol (10 mL). Water was added and the mixture was extracted by ethyl acetate (5×250 mL). The extracts were dried over $MgSO_4$ and evaporated. The residue (29 g) was subjected to column chromatography (silica gel, 1000 g; 0.5% of methanol in chloroform) yielding 8.4 g of **3a** (29%); colorless crystals; mp 68–71°C. ^{1}H NMR δ (ppm), $CDCl_3$: 1.06–1.74 (m, 10H); 2.13 (bs, 1H); 3.48–3.81 (m, 18H). FAB MS *m/z* (%): 316 ([M+H]$^+$, 100%). Anal. calcd for $C_{16}H_{29}NO_5{\cdot}H_2O$: C, 57.63; H, 9.37; N, 4.20. Found: C, 57.61; H, 9.47; N, 4.17.

4.2.2. Spiro-16-crown-5 (3b). Solutions of diol **1** (10 g, 50 mmol) in dry dioxane (300 mL) and ditosylate **2b** (25 g, 50 mmol) in dry dioxane (300 mL) were added slowly (30 mL h^{-1}) by dual syringe pump to the intensively stirred suspension of freshly powdered KOH (13.2 g, 200 mmol) in dry dioxane (300 mL) at 80°C. After heating and stirring another 10 h and subsequent cooling the deposited salts were filtered off, washed with dioxane (200 mL) and the solvent was evaporated. The residue was subjected to column chromatography (silica gel; 700 g; 1.5% of methanol in chloroform) yielding 6.82 g of **3b** (38%); oil. ^{1}H NMR δ (ppm), $CDCl_3$: 1.16–1.70 (m, 10H); 2.43 (bs, 1H); 3.48–3.65 (m, 18H). FAB MS *m/z* (%): 360 ([M+H]$^+$,

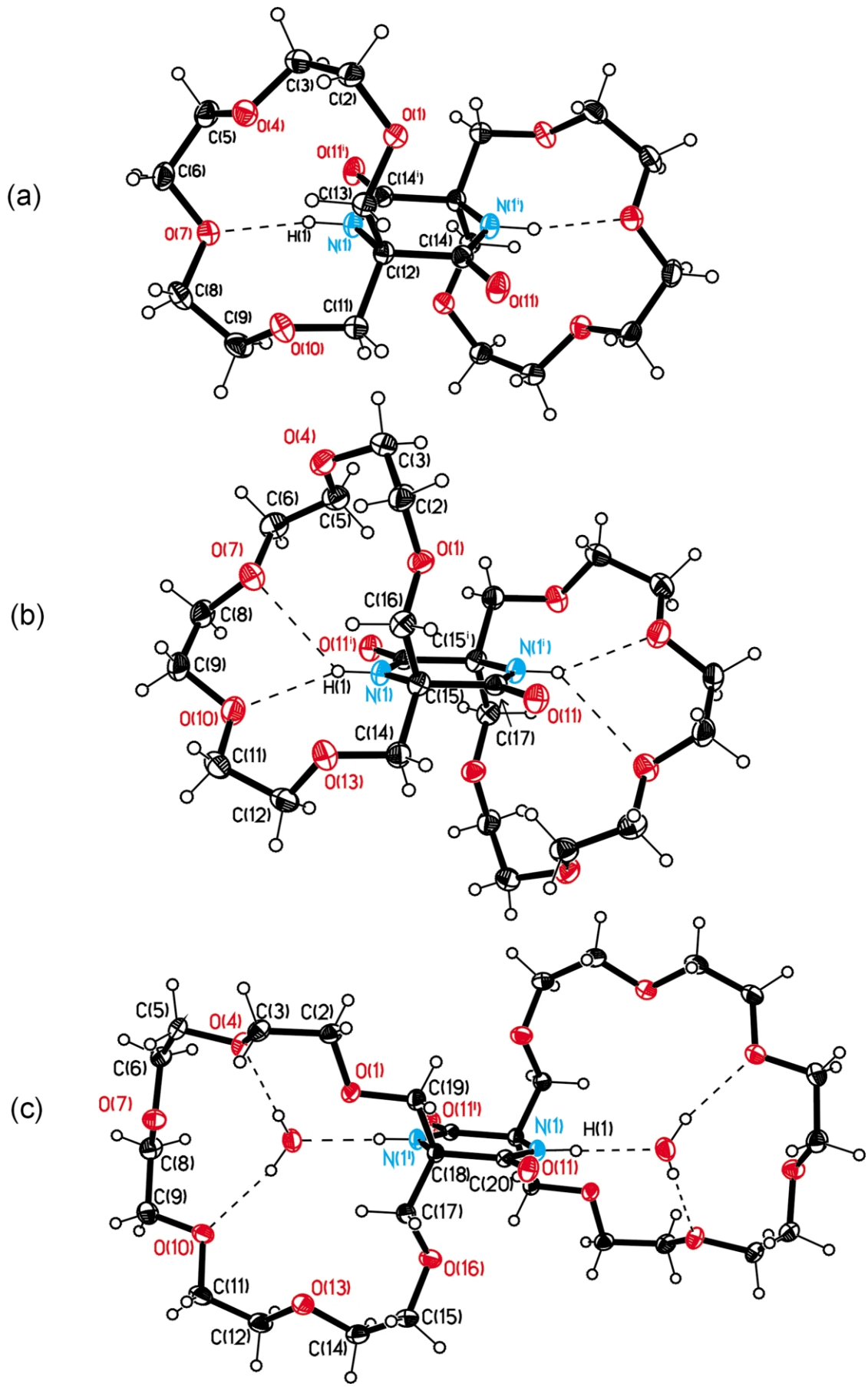

Figure 4. ORTEP drawings of the molecular structure of dioxopiperazines **12a** (a), **12b** (b) and **12c** (c) with atom numbering (ellipsoids: 50% probability) and intramolecular hydrogen bonds (dashed lines).

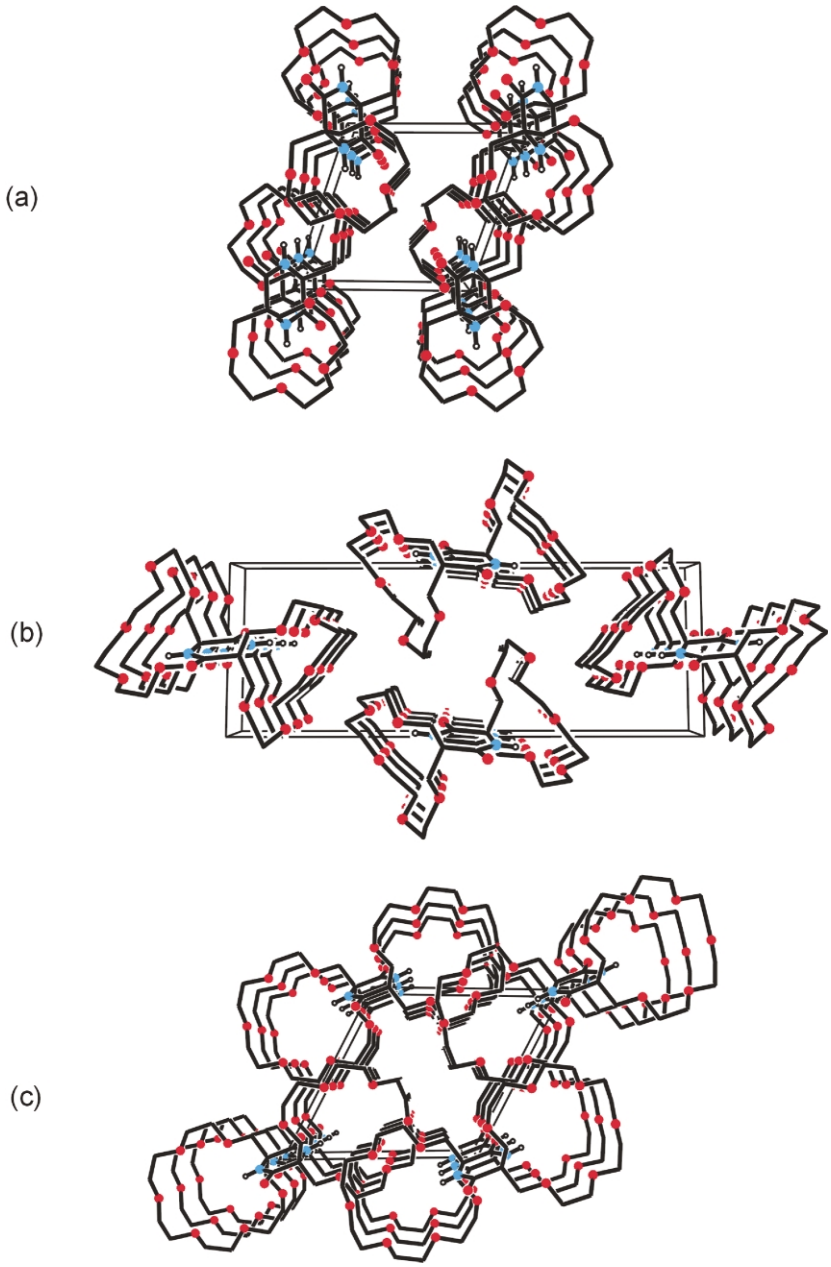

Figure 5. Perspective views on the crystal packing of the dioxopiperazines **12a** (a), **12b** (b) and **12c** (c). In (c), water molecules occupying the crown ring cavities have been omitted.

100%). Anal. calcd for $C_{18}H_{33}NO_6$: C, 60.14; H, 9.26; N, 3.90. Found: C, 59.87; H, 9.31; N, 3.37.

4.2.3. Spiro-19-crown-6 (3c). Prepared analogously to **3b** starting from penta(ethylene glycol)ditosylate **2c**. Yield 9.89 g (49%); oil. ^{1}H NMR δ (ppm), $CDCl_3$: 1.08–1.73 (m, 10H); 2.12 (bs, 1H); 3.50–3.80 (m, 26H). FAB MS *m*/*z* (%): 404 ($[M+H]^+$, 100%); 426 ($[M+Na]^+$, 6%). Anal. calcd for $C_{20}H_{37}NO_7$: C, 59.53; H, 9.24; N, 3.47. Found: C, 59.12; H, 9.46; N, 3.41.

4.2.4. Hydrolysis of spiro-crowns (3a–c) and in situ *N*-CBz protection of resulting amino alcohols (4a–c). 3 M HCl (150 mL) was added to an appropriate spiro-crown **3a–c** (12 mmol) and the mixture was stirred and heated at 55°C for 5 h. Hydrochloric acid was evaporated, the resulting amino alcohol hydrochloride **4a–c** (12 mmol) was dissolved in the 1:1 mixture of dioxane and water (200 mL) and sodium hydrogen carbonate (12.6 g, 150 mmol) was added. Benzyl chloroformate (2.2 mL, 15 mmol, in 25 mL of dioxane) was added slowly during 2 h under vigorous stirring at 0°C and the reaction mixture was stirred another 2 h at ambient temperature. Dioxane was evaporated, the residue was dissolved in water and extracted with ethyl acetate (5×200 mL). The organic layer was dried over $MgSO_4$, evaporated and the crude product was purified by column chromatography (500 g of silica gel, 0.5–2% of methanol in chloroform).

N-Cbz-amino alcohol **5a**: yield 3.32 g (75%); oil. ^{1}H NMR δ (ppm), $CDCl_3$: 3.63–3.87 (m, 19H); 5.06 (s, 2H); 5.65 (bs, 1H); 7.33–7.37 (m, 5H). FAB MS *m*/*z* (%): 370 ($[M+H]^+$,

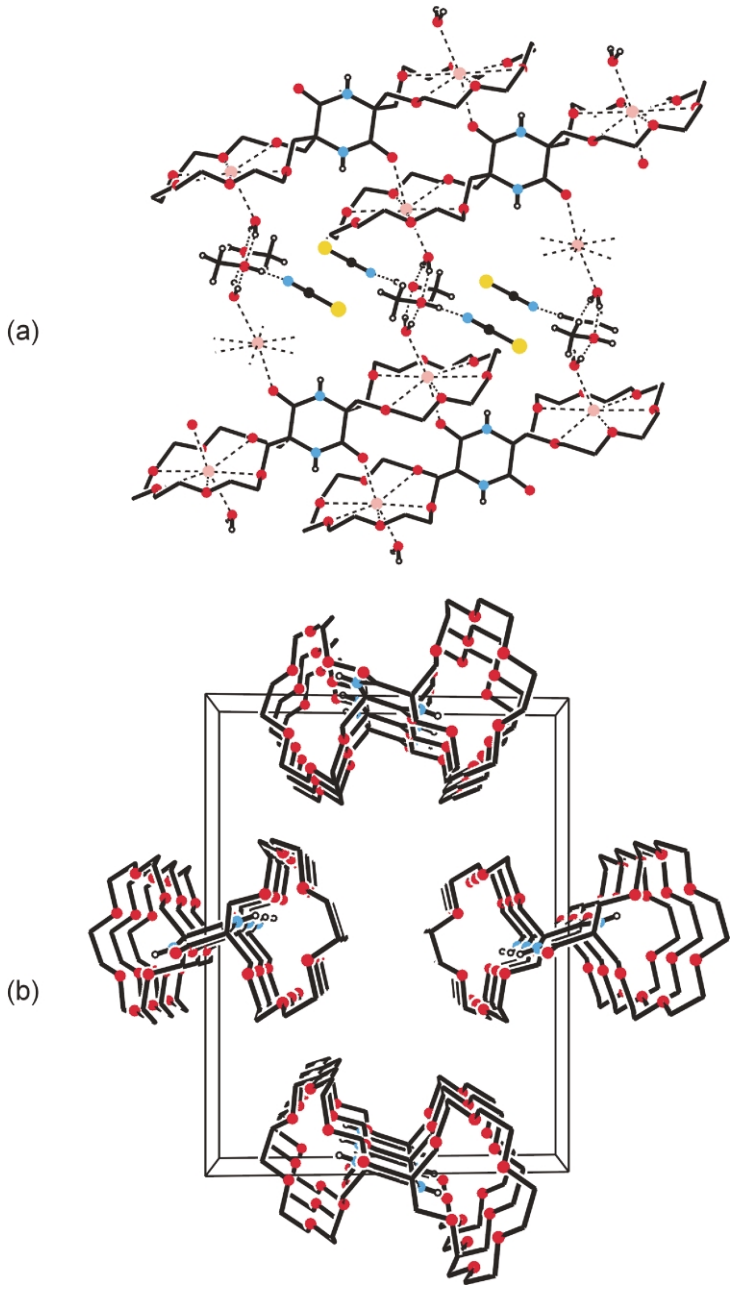

Figure 6. Detailed scheme of intermolecular contacts in the crystal structure of solvated 1:1 complex **12c**·KSCN (a) and the packing of **12c** (b). Potassium and sulfur atoms are represented with pink and yellow circles, respectively.

75%). Anal. calcd for $C_{18}H_{27}NO_7$: C, 58.53; H, 7.37; N, 3.79. Found: C, 58.61; H, 7.75; N, 3.94.

N-Cbz-amino alcohol **5b**: yield 3.03 g (61%); oil. ^{1}H NMR δ (ppm), $CDCl_3$: 3.55–3.87 (m, 23H), 5.07 (s, 2H); 5.80 (bs, 1H); 7.34–7.36 (m, 5H). FAB MS *m*/*z* (%): 414 ($[M+H]^+$, 75%), 436 ($[M+Na]^+$, 48%). Anal. calcd for $C_{20}H_{31}NO_8 \cdot H_2O$: C, 55.67; H, 7.71; N, 3.24. Found: C, 55.94; H, 7.78; N, 3.28.

N-Cbz-amino alcohol **5c**: 4.47 g (79%); oil. ^{1}H NMR δ (ppm), $CDCl_3$: 3.60–3.85 (m, 27H), 5.07 (s, 2H); 5.76 (bs, 1H); 7.34–7.36 (m, 5H). FAB MS *m*/*z* (%): 458 ($[M+H]^+$, 42%), 350 (100%.). Anal. calcd for $C_{22}H_{35}NO_9 \cdot 0.5H_2O$: C, 56.63; H, 7.78; N, 3.00. Found: C, 56.96; H, 7.82; N, 2.99.

4.2.5. Oxidation of *N*-Cbz-protected amino alcohols (5a–c). *N*-Cbz-amino alcohol **5a**–**c** (12 mmol) dissolved in H_2O (80 mL) and CH_3CN (50 mL) was treated with $NaHCO_3$ (5.5 g, 65 mmol) and TEMPO (0.5 g, 3.2 mmol). Aqueous solution of sodium hypochlorite (8.5 mL) was added in several portions under stirring at room temperature and the progress of the reaction was followed by TLC. After 3–5 h, acetonitrile was evaporated and the residue was extracted with hexane (3×150 mL). The aqueous layer was acidified by 3 M aqueous HCl, extracted with ethyl acetate (6×150 mL) and the extracts were dried over magnesium sulfate and evaporated. The crude product was purified by crystallization (**6a**, **c**) or column chromatography on silica gel (**6b**).

N-Cbz-protected amino acid **6a**: 3.3 g (72%); colorless crystals; mp 153°C. ^{1}H NMR δ (ppm), DMSO-d_6: 3.34–3.84

(m, 16H); 4.99 (s, 2H); 7.34 (m, 5H); 7.54 (bs, 1H); 12.44 (bs, 1H). FAB MS *m/z* (%): 384 ($[M+H]^+$, 35%), 340 (40%). Anal. calcd for $C_{18}H_{25}NO_8$: C, 56.36; H, 6.57; N, 3.65. Found: C, 56.45; H, 6.73; N, 3.59.

N-Cbz-protected amino acid **6b**: 4.1 g (80%); oil. ^{1}H NMR δ (ppm), DMSO-d_6: 3.36–3.84 (m, 20H); 4.98 (s, 2H); 6.98 (bs, 1H); 7.34 (m, 5H). FAB MS *m/z* (%): 428 ($[M+H]^+$, 35%). Anal. calcd for $C_{20}H_{29}NO_9 \cdot H_2O$: C, 53.92; H, 7.01; N, 3.14. Found: C, 53.78; H, 6.95; N, 2.94.

N-Cbz-protected amino acid **6c**: 4.5 g (70%); colorless crystals; mp 96–97°C. ^{1}H NMR δ (ppm), DMSO-d_6: 3.36–3.84 (m, 20H); 4.98 (s, 2H); 6.98 (bs, 1H); 7.34 (m, 5H). FAB MS *m/z* (%): 494 ($[M+Na]^+$, 100%); 516 ($[M+2Na]^+$, 54%). Negative ion FAB MS *m/z* (%): 470 ($[M-H]^-$, 100%). Anal. calcd for $C_{22}H_{33}NO_{10}$: C, 56.04; H, 7.06; N, 2.97. Found: C, 56.02; H, 7.23; N, 2.91.

4.2.6. Hydrogenolysis of *N*-Cbz-amino acids (6a–c). *N*-Cbz-protected amino acid **6a–c** (0.5 mmol) was dissolved in methanol, 10% Pd/C catalyst (50 mg) was added and hydrogen was bubbled through the reaction mixture for 3 h. After standing overnight under hydrogen, the catalyst was filtered off and the solvent was evaporated. The residue was crystallized from the mixture of methanol and diethyl or diisopropyl ether.

Free amino acid **7a**: yield 0.115 g (92%); colorless crystals; mp 192–196°C. ^{1}H NMR δ (ppm), DMSO-d_6: 3.35–3.85 (m, 16H); 7.42 (bs, 2H). FAB MS *m/z* (%): 250 ($[M+H]^+$, 100%). Anal. calcd for $C_{10}H_{19}NO_6 \cdot H_2O$: C, 44.94; H, 7.92; N, 5.24. Found: C, 44.72; H, 7.95; N, 5.11.

Free amino acid **7b**: yield 0.130 g (88%); colorless crystals; mp 135–137°C. ^{1}H NMR δ (ppm), DMSO-d_6: 3.30–3.82 (m, 20H); 7.20 (bs, 2H). FAB MS *m/z* (%): 280 ($[M+H]^+$, 100%). Anal. calcd for $C_{12}H_{23}NO_7$: C, 49.14; H, 7.90; N, 4.78. Found: C, 49.03; H, 7.75; N, 4.90.

Free amino acid **7c**: yield 0.155 g (91%); colorless crystals; mp 163–166°C. ^{1}H NMR δ (ppm), DMSO-d_6: 3.44–3.78 (m, 24H); 7.13 (bs, 2H). FAB MS *m/z* (%): 338 ($[M+H]^+$, 100%). Anal. calcd for $C_{14}H_{27}NO_8$: C, 49.69; H, 8.04; N, 4.14. Found: C, 49.53; H, 8.12; N, 4.11.

4.2.7. Methyl esters of *N*-Cbz-amino acids (8a–c). *N*-Cbz-protected amino acid **6a–c** (2 mmol) was dissolved in dry dichloromethane (30 mL) and an excess of diazomethane in diethyl ether was slowly added. After 15 min the solvents were evaporated and the residue was dried in vacuo.

8a: yield 0.79 g (99%); oil. ^{1}H NMR δ (ppm), $CDCl_3$: 3.52–3.80 (m, 16H); 3.93 (s, 3H); 5.09 (s, 2H); 5.51 (bs, 1H); 7.34 (m, 5H). FAB MS *m/z* (%): 398 ($[M+H]^+$, 100%). Anal. calcd for $C_{19}H_{27}NO_8$: C, 57.42; H, 6.85; N, 3.52. Found: C, 57.31; H, 6.79; N, 3.54.

8b: yield 0.88 g (99%); oil. ^{1}H NMR δ (ppm), $CDCl_3$: 3.60–3.70 (m, 16H); 3.87 (s, 3H); 3.90–4.10 (m, 4H) 5.11 (s, 2H); 6.03 (bs, 1H); 7.34 (m, 5H). FAB MS *m/z* (%): 464 ($[M+Na]^+$, 100%). Anal. calcd for $C_{21}H_{31}NO_9$: C, 57.13; H, 7.08; N, 3.17. Found: C, 56.89; H, 6.91; N, 3.01.

8c: yield 0.96 g (99%); oil. ^{1}H NMR δ (ppm), $CDCl_3$: 3.56–3.70 (m, 20H); 3.76 (s, 3H);3.90–4.07 (m, 4H) 5.10 (s, 2H); 6.08 (bs, 1H); 7.34 (m, 5H). FAB MS *m/z* (%): 486 ($[M+H]^+$, 15%); 508 ($[M+Na]^+$, 100%). Anal. calcd for $C_{23}H_{35}NO_{10} \cdot H_2O$: C, 54.86; H, 7.41; N, 2.78. Found: C, 55.08; H, 7.31; N, 2.88.

4.2.8. Hydrogenolysis of *N*-Cbz-protected esters (8a–c). *N*-Cbz-protected amino acid methyl ester **8a–c** (2 mmol) was dissolved in methanol (30 mL), 10% Pd/C catalyst (50 mg) was added and the reaction mixture was stirred under hydrogen for 5–10 h until the deprotection was complete (TLC). The catalyst was filtered off, methanol was evaporated and the oily product was dried in vacuo.

Deprotected ester **9a**: 0.52 g (99%); oil. ^{1}H NMR δ (ppm), DMSO-d_6: 3.45–3.72 (m, 12H); 3.76 (s, 3H); 3.91 (dd, 4H); 8.68 (bs, 2H). FAB MS *m/z* (%): 264 ($[M+H]^+$, 100%). HRMS (FAB) calcd for $C_{11}H_{21}NO_6$: 264.1447. Found: 264.1461.

Deprotected ester **9b**: 0.65 g (94%); oil. ^{1}H NMR δ (ppm), DMSO-d_6: 3.60–4.39 (m, 23H); 9.44 (bs, 2H). FAB MS *m/z* (%): 308 ($[M+H]^+$, 100%); HRMS (FAB) calcd for $C_{13}H_{25}NO_7$: 308.1709. Found: 308.1668.

Deprotected ester **9c**: 0.69 g (98%); oil. ^{1}H NMR δ (ppm), DMSO-d_6: 3.28–4.02 (m, 27H); 8.68 (bs, 2H). FAB MS *m/z* (%): 352 ($[M+H]^+$, 100%); HRMS (FAB) calcd for $C_{15}H_{29}NO_8$: 352.1971. Found: 352.1905.

4.2.9. *N*-Cbz-protected dipeptides (10a–c). Free methyl ester **9a–c** (1 mmol), *N*-Cbz-protected amino acid **6a–c** (1 mmol) and benzotriazol-1-yl-oxy-tripyrrolidinophosphonium hexafluorophosphate (0.6 g, 1.15 mmol) were dissolved in diisopropylethyl amine (3 mL) and dry dichloromethane (3 mL) and the reaction mixture was stirred gently at rt for 5 days. Solvents were taken off and the crude residue was subjected to column chromatography (silica gel; chloroform–methanol 97:3).

10a: yield 0.46 g (73%); colorless crystals; mp 117–118°C. ^{1}H NMR δ (ppm), $CDCl_3$: 3.60–4.18 (m, 35H); 5.05 (s, 2H); 5.81 (bs, 1H); 7.33 (m, 5H); 7.82 (bs, 1H). FAB MS *m/z* (%): 629 ($[M+H]^+$, 100%); HRMS (FAB) calcd for $C_{29}H_{45}N_2O_{13}$: 629.2921. Found: 629.2912.

10b: yield 0.44 g, (61%); oil. ^{1}H NMR δ (ppm), $CDCl_3$: 3.55–4.20 (m, 43H); 5.07 (s, 2H); 6.17 (bs, 1H); 7.33 (m, 5H); 7.51 (bs, 1H). FAB MS *m/z* (%): 717 ($[M+H]^+$, 29%); 739 ($[M+Na]^+$, 100%; HRMS (FAB) calcd for $C_{33}H_{53}N_2O_{15}$: 717.3446. Found: 717.3342.

10c: yield 0.50 g, (62%); oil. ^{1}H NMR δ (ppm), $CDCl_3$: 3.55–4.18 (m, 51H); 5.09 (s, 2H); 6.18 (bs, 1H); 7.34 (m, 5H); 7.61 (bs, 1H). FAB MS *m/z* (%): 805 ($[M+H]^+$, 68%); 827 ($[M+Na]^+$, 100%); HRMS (FAB) calcd for $C_{37}H_{61}N_2O_{15}$: 805.3970. Found: 805.3932.

4.2.10. Deprotected dipeptides (11a–c). Prepared by hydrogenolysis of **10a–c** (0.5 mmol) analogously as described for the amino acid methyl esters **9a–c**.

Table 2. Crystal data of amino acids **7a–c**, measurement and refinement details

	7a	**7b·NaCl**	**7c**
Formula	$C_{10}H_{19}NO_6{\cdot}CH_3OH$	$C_{12}H_{23}NO_7{\cdot}0.8CH_3OH{\cdot}2.2H_2O{\cdot}NaCl$	$C_{14}H_{27}NO_8{\cdot}CH_3OH$
Crystal system	Tetragonal	Monoclinic	Monoclinic
Space group	$P4_2/n$ (No. 86)	$P2_1/c$ (No. 14)	$P2_1/c$ (No. 14)
a (Å)	11.5980(1)	10.3940(2)	9.8810(2)
b (Å)	11.5980(1)	13.1140(2)	19.3250(5)
c (Å)	21.3130(3)	14.5290(3)	10.0020(2)
β (°)		100.6320(11)	103.1250(18)
Z	8	4	4
V (Å^3)	2866.89(5)	1946.40(6)	1859.99(7)
D_c (g cm^{-3})	1.303	1.423	1.3191(1)
Crystal size (mm)	0.8×0.7×0.5	0.6×0.4×0.37	0.6×0.4×0.37
μ (mm^{-1})	0.108	0.268	0.108
h range	−15, 15	−13, 13	−12, 12
k range	−10, 10	−17, 17	−25, 25
l range	−27, 27	−18, 18	−12, 12
Reflections measured	37350	30625	26871
-independent (R_{int}[a])	3233(0.0265)	4452(0.030)	4260
-observed [$I>2\sigma(I)$]	2698	3862	3299
No. of parameters	189	256	243
GOF[b]	1.044	1.097	1.047
R[c], wR[c]	0.041, 0.113	0.039, 0.114	0.043, 0.095
$\Delta\rho$ (e Å^{-3})	0.273, −0.238	1.000, −0.322	0.301, −0.216

[a] $R_{int}=\sum|F_o^2-F_{o,mean}^2|/\sum F_o^2$.
[b] GOF$=[\sum(w(F_o^2-F_c^2)^2)/(N_{diffrs}-N_{params})]^{1/2}$ for all data.
[c] $R(F)=\sum\|F_o|-|F_c\|/\sum|F_o|$ for observed data, $wR(F^2)=[\sum(w(F_o^2-F_c^2)^2)/(\sum w(F_o^2)^2)]^{1/2}$ for all data.

11a: yield 0.24 g (97%); oil. ^{1}H NMR δ (ppm), $CDCl_3$: 3.40–4.20 (m, 35H); 8.66 (bs, 1H); 8.97 (bs, 2H). FAB MS m/z (%): 495 ([M+H]$^+$, 100%). HRMS (FAB) calcd for $C_{21}H_{39}N_2O_{11}$: 495.2554. Found: 495.2509.

11b: yield 0.27 g (93%); oil. ^{1}H NMR δ (ppm), $CDCl_3$: 3.41–4.19 (m, 43H). FAB$^+$ MS m/z (%): 583 ([M+H]$^+$, 100%). HRMS (FAB) calcd for $C_{25}H_{47}N_2O_{13}$: 583.3078. Found: 583.3055.

11c: yield 0.32 g (92%); oil. ^{1}H NMR δ (ppm), $CDCl_3$: 3.45–4.08 (m, 51H). FAB MS m/z (%): 671 ([M+H]$^+$, 100%). HRMS (FAB) calcd. for $C_{29}H_{55}N_2O_{15}$: 671.3602. Found: 671.3567.

4.2.11. Dioxopiperazines (12a–c). Peptide esters **11a–c** (0.25 mmol) were dissolved in sat. methanolic ammonia (25 mL) and left at rt for 24 h. The mixture was taken to dryness and the crude product was crystallized from a

Table 3. Crystal data of dioxopiperazines **12a–c**, measurement and refinement details

	12a	**12b**	**12c**	**12c·KSCN**
Formula	$C_{20}H_{34}N_2O_{10}$	$C_{24}H_{42}N_2O_{12}$	$C_{28}H_{50}N_2O_{14}{\cdot}2H_2O$	$C_{28}H_{50}N_2O_{14}{\cdot}2H_2O{\cdot}2CH_3OH{\cdot}2KSCN$
Crystal system	Triclinic	monoclinic	triclinic	Monoclinic
Space group	P-1 (No. 2)	$P2_1/c$ (No. 14)	P-1 (No. 2)	$P2_1/c$ (No. 14)
a (Å)	8.1990(2)	7.9300(2)	8.0950(2)	8.2430(1)
b (Å)	8.6000(2)	21.6780(4)	10.7640(2)	19.0730(3)
c, Å	8.6560(2)	8.2290(1)	11.2780(3)	14.6010(1)
α (°)	70.9190(16)		115.7030(15)	
β (°)	75.5340(16)	104.5510(10)	105.8550(14)	97.2750(18)
χ (°)	86.1190(18)		91.4070(14)	
Z	1	2	1	2
V (Å^3)	558.46(2)	1369.24(5)	840.10(4)	2277.07(13)
D_c (g cm^{-3})	1.375	1.335	1.334	1.361
Crystal size (mm)	0.37×0.3×0.25	0.45×0.3×0.3	0.6×0.5×0.5	0.5×0.1×0.05
μ (mm^{-1})	0.110	0.107	0.109	0.372
h range	−10, 10	−10, 10	−10, 10	−9, 9
k range	−11, 11	−27, 28	−13, 13	−22, 22
l range	−10, 11	−10, 10	−14, 13	−17, 17
Reflections measured	11028	23113	13142	33086
-independent (R_{int}[a])	2560(0.029)	3118(0.032)	3821(0.027)	4014(0.071)
-observed [$I>2\sigma(I)$]	2278	2669	3536	2989
No. of parameters	150	176	221	279
GOF[b]	1.028	1.058	1.046	1.025
R[c], wR[c]	0.034, 0.088	0.036, 0.093	0.031, 0.078	0.041, 0.095
$\Delta\rho$ (e Å^{-3})	0.310, −0.200	0.294, −0.259	0.343, −0.201	0.389, −0.219

[a] $R_{int}=\sum|F_o^2-F_{o,mean}^2|/\sum F_o^2$.
[b] GOF$=[\sum(w(F_o^2-F_c^2)^2)/(N_{diffrs}-N_{params})]^{1/2}$ for all data.
[c] $R(F)=\sum\|F_o|-|F_c\|/\sum|F_o|$ for observed data, $wR(F^2)=[\sum(w(F_o^2-F_c^2)^2)/(\sum w(F_o^2)^2)]^{1/2}$ for all data.

Table 4. Parameters of hydrogen bonds in the crystal structures

Compound	Specification D–H···A	Distances (Å)			Bond angle (°) D H A
		D–H	H···A	D···A	
7a	N(1)–H(1B)···O(12)[a]	0.899(17)	2.004(17)	2.8415(13)	154.4(14)
	N(1)–H(1A)···O(7)	0.890(18)	2.002(18)	2.8679(15)	164.1(14)
	N(1)–H(1A)···O(4)	0.890(18)	2.583(16)	3.1519(15)	122.5(12)
	N(1)–H(1C)···O(12)[b]	0.898(17)	1.883(18)	2.7683(14)	168.4(15)
	O(15)–H(15)[MeOH]···O(11)	0.94(3)	1.84(3)	2.7281(18)	157(2)
7b·NaCl	N(1)–H(1A)···O(4)[c]	0.89	2.19	3.0630(17)	166.7
	N(1)–H(1B)···O(18)[d]	0.89	1.92	2.798(2)	170.5
	N(1)–H(1C)···Cl(1)	0.89	2.41	3.2811(13)	165.2
	O(1W)–H(11W)···O(11)[e]	0.87	1.95	2.8158(17)	169.1
	(1W)–H(12W)···Cl(1)[f]	0.89	2.38	3.2434(13)	164.8
	O(2W)–H(21W)···O(12)[d]	0.88	1.94	2.815(2)	170.2
	O(2W)–H(22W)···Cl(1)	0.99	2.24	3.2221(18)	175.5
	O(18)–H(18)[MeOH]···O(12)	0.84(3)	2.03(3)	2.761(2)	146(2)
7c	N(1)–H(1A)···O(7)	0.887(18)	2.139(18)	2.9329(16)	148.7(14)
	N(1)–H(1B)···O(13)	0.90(2)	2.48(2)	3.3246(17)	157.2(16)
	N(1)–H(1C)···O(12)[g]	0.945(18)	1.762(19)	2.6983(15)	170.2(15)
	O(21)–H(21)·[MeOH]···O(11)	0.87(2)	1.89(2)	2.7543(16)	174(2)
12a	N(1)–H(1)···O(7)	0.888(16)	2.8855(12)	2.007(16)	169.7(13)
12b	N(1)–H(1)···O(7)	0.866(16)	2.634(16)	3.2866(13)	133.0(12)
	N(1)–H(1)···O(10)	0.866(16)	2.241(16)	3.0571(13)	157.0(13)
12c	N(1)–H(1)···O(1W)[h]	0.872(14)	2.001(14)	2.8679(11)	173.2(12)
	O(1W)–H(1W)···O(10)	0.833(18)	2.130(18)	2.9403(10)	164.1(15)
	O(1W)–H(2W)···O(4)	0.851(18)	2.114(18)	2.9617(10)	173.3(15)
	O(1W)–H(2W)···O(1)	0.851(18)	2.616(16)	3.0786(10)	115.4(13)
12c·KSCN	N(1)–H(1)···O(7)[i]	0.77(2)	2.57(2)	3.317(2)	164(2)
	O(1M)–H(1M)···N(1T)[NCS^-]	0.97(4)	1.72(4)	2.680(3)	172(4)
	O(1W)–H(1W)···O(1M)	0.86(4)	1.98(4)	2.820(3)	166(4)
	O(1W)–H(1W)···O(1M)	0.86(4)	1.98(4)	2.820(3)	166(4)

[a] Symmetry transformations used to generate equivalent atoms: $y, -x+3/2, -z+1/2$.
[b] Symmetry transformations used to generate equivalent atoms: $-y+3/2, x, -z+1/2$.
[c] Symmetry transformations used to generate equivalent atoms: $x, -y+1/2, z+1/2$.
[d] Symmetry transformations used to generate equivalent atoms: $-x, y+1/2, -z+1/2$.
[e] Symmetry transformations used to generate equivalent atoms: $-x, -y, -z$.
[f] Symmetry transformations used to generate equivalent atoms: $x, -y+1/2, z-1/2$.
[g] Symmetry transformations used to generate equivalent atoms: $x, -y+1/2, z+1/2$.
[h] Symmetry transformations used to generate equivalent atoms: $-x, -y+2, -z$.
[i] Symmetry transformations used to generate equivalent atoms: $-x+1, -y+1, -z$.

mixture of methanol–diethyl ether or methanol–diisopropyl ether.

12a: yield 0.046 g (40%); colorless crystals; mp 264–265°C. ^{1}H NMR δ (ppm), $CDCl_3$: 3.44–3.96 (m, 28H); 4.16 (d, J=11.0 Hz, 8H); 8.47 (s, 2H). FAB MS m/z (%): 463 ($[M+H]^+$, 100%). Anal. calcd for $C_{20}H_{34}N_2O_{10}\cdot H_2O$: C, 50.00; H, 7.55; N, 5.83. Found: C, 50.32; H, 7.35; N, 5.69.

12b: yield 0.085 g (62%); colorless crystals; mp 155–157°C. ^{1}H NMR δ (ppm), $CDCl_3$: 3.50–3.96 (m, 36H); 3.88 (d, J=9.8 Hz, 8H); 7.69 (s, 2H). FAB MS m/z (%): 551 ($[M+H]^+$, 47%) 573 ($[M+Na]^+$, 100%). Anal. calcd for $C_{24}H_{342}N_2O_{12}\cdot H_2O$: C, 50.69; H, 7.80; N, 4.93. Found: C, 50.37; H, 7.62; N, 4.86.

12c: yield 0.102 g (64%); colorless crystals; mp 112–113°C. ^{1}H NMR δ (ppm), $CDCl_3$: 3.56–3.92 (m, 36H); 3.83 (d, J=9.2 Hz, 8H); 7.19 (s, 2H). FAB MS m/z (%): 638 ($[M+H]^+$, 100%). Anal. calcd for $C_{28}H_{50}N_2O_{14}$: C, 52.65; H, 7.89; N, 4.39. Found: C, 52.68; H, 8.03; N, 4.22.

4.3. FAB MS study of complexation of alkali metal cations with amino acids (7a–c)

An appropriate ligand **7a–c** (1×10^{-2} μmol) and an equimolar mixture of Li^+, Na^+, K^+, Rb^+ and Cs^+ salt (1×10^{-2} μmol of each) in 50% aqueous methanol (2 μL) were added to thioglycerol–glycerol matrix. Complex formation was monitored by FAB MS under acidic (presence of 5×10^{-1} μmol HCl), neutral (chloride counterion) as well as basic (hydroxide counterion) conditions.

4.4. X-Ray study

Crystals of **7a**, **7b**·NaCl, **7c**, **12a–c** and **12c**·KSCN suitable for X-ray structure determination were obtained by a slow diffusion of diisopropyl ether to the corresponding methanolic solution. Data were collected at 150(2) K on a Nonius KappaCCD diffractometer using Mo Kα radiation (λ=0.71073 Å) and a graphite monochromator. The structures were solved by direct methods (SIR92[9]). All reflections were used in the structure refinement based on F^2 by full-matrix least-squares technique (SHELXL97[10]).

Hydrogen atoms were mostly localized on a difference Fourier map, however to ensure uniformity of treatment of all crystals, all hydrogens bonded to carbon atoms were recalculated into ideal positions (riding model) and assigned temperature factors $H_{iso}(H)=1.2U_{eq}(C)$ or $1.5U_{eq}(C)$ for the methyl moiety. Absorption corrections were neglected; $(\Delta/\delta)_{max}<0.001$ was attained in the last cycle of refinement of all structures. Crystallographic data for individual structures are summarized in Tables 2–4. Crystallographic data (excluding structure factors) for the structures in this paper have been deposited with the Cambridge Crystallographic Data Centre as supplementary publication numbers CCDC: **7a** No. 184770; **7b**·NaCl No. 184771; **7c** No. 184772; **12a** No. 184773; **12b** No. 184774; **12c** No. 184933; **12c**·KSCN No. 184775. Copies of the data can be obtained, free of charge, on application to CCDC, 12 Union Road, Cambridge, CB2 1EZ, UK [fax: +44-1223-336033 or e-mail: deposit@ccdc.cam.ac.uk].

Acknowledgements

The financial support of the Grant Agency of the Czech Republic (203/00/0137 and 203/00/0138) is warmly acknowledged. I. C. thanks for the instrument-providing grant (203/99/M037) and for the access to the CDS (203/99/0067).

References

1. (a) Izatt, R. M.; Pawlak, K.; Bradshaw, J. S.; Bruening, R. L. *Chem. Rev.* **1991**, *91*, 1721–2085. (b) Bradshaw, J. S.; Izatt, R. M. *Acc. Chem. Res.* **1997**, *30*, 338–345.
2. (a) Berthet, M.; Sonveax, E. *Biopolymers* **1986**, *25*, 189–204. (b) Mazaleyrat, J.-P.; Gaucher, A.; Goubard, Y.; Šavrda, J.; Wakselman, M. *Tetrahedron Lett.* **1997**, *38*, 2091–2095. (c) Kraus, T.; Buděšínský, M.; Závada, J.; Císařová, I. *Angew. Chem. Int. Ed.* **2002**, *41*, 1715–1717.
3. (a) Zaworotko, M. *Angew. Chem. Int. Ed.* **2000**, *39*, 3052–3054. (b) Bong, D. T.; Clerk, T. D.; Granja, J. R.; Ghadiri, M. R. *Angew. Chem. Int. Ed.* **2001**, *40*, 988–1011. (c) Eddaoudi, M.; Moler, D. B.; Li, H.; Chen, B.; Reineke, T.; O'Keeffe, M.; Yaghi, O. M. *Acc. Chem. Res.* **2001**, *34*, 319–329. (d) Holý, P.; Závada, J.; Císařová, I.; Podlaha, J. *Tetrahedron: Asymmetry* **2001**, *12*, 3035–3045.
4. Pierce, J. S.; Lunsford, C. D.; Raiford, Jr. R. W.; Rush, J. L.; Riley, D. W. *J. Am. Chem. Soc.* **1951**, *73*, 2595–2596.
5. Kraus, T.; Buděšínský, M.; Závada, J. *Eur. J. Org. Chem.* **2000**, 3133–3137.
6. (a) McDonald, J. C.; Whitesides, G. M. *Chem. Rev.* **1994**, *94*, 2383–2420. (b) Palacin, S.; Chin, D. N.; Simanek, E. E.; McDonald, J. C.; Whitesides, G. M.; McBride, M. T.; Palmore, G. T. R. *J. Am. Chem. Soc.* **1997**, *119*, 11807–11816. (c) Chin, D. N.; Palmore, G. T. R.; Whitesides, G. M. *J. Am. Chem. Soc.* **1999**, *121*, 2115–2122.
7. Palmore, G. T. R.; McBride, M. T. *Chem. Commun.* **1998**, 145–146.
8. Chen, Y.; Baker, G. L. *J. Org. Chem.* **1999**, *64*, 6870–6873.
9. Altomare, A.; Cascarano, G.; Giacovazzo, C.; Guagliardi, A.; Burla, M. C.; Polidori, G.; Camalli, M. *J. Appl. Crystallogr.* **1994**, *27*, 435.
10. Sheldrick, G. M. *SHELXL-97*: *A Program for Crystal Structure Refinement*; University of Göttingen: Germany, 1997.